



## Research article

# Dust detection and cleanliness assessment based on S-YOLOv5s for NPP reactor containment wall-climbing cleaning robot

Li-Wen Chen<sup>a</sup>, Jing Zhu<sup>a,\*</sup>, Huanghui Zhang<sup>b</sup>, Yang Liu<sup>c</sup>, Chun-yu Liu<sup>a</sup><sup>a</sup> School of Computer Science, School of Electrical, Electronics & Physics, Fujian University of Technology, Fuzhou, Fujian, China<sup>b</sup> Electricity Department, Fujian Metrology Institute, Fuzhou, Fujian, China<sup>c</sup> Inner Mongolia Yili Industrial Group Co. Hohhot, Inner Mongolia, China

## ARTICLE INFO

## Keywords:

Dust detection algorithm  
Lightweight  
Cleanliness assessment  
Reactor containment cleaning  
Wall-climbing cleaning robot

## ABSTRACT

NPP reactor containment dust can easily turn into radioactive dust, endangering staff health and the environment. However, the nuclear reactor containment wall-climbing cleaning robot cleans blindly without the ability to clean the dust in a timely and thoroughly. In this paper, ShuffleNetV2-YOLOv5s (S-YOLOv5s) model is proposed to solve the problem of wall-climbing robots unable to detect different categories of dust in time. The use of ShuffleNetV2 in the backbone of the network not only ensures a large number of characterized channels and a large network capacity, but also reduces the complexity of the model; SIoU is chosen for the loss function to improve the model accuracy. Then, planar cleaning index (PCI) is proposed by combining the results of S-YOLOv5s to evaluate whether the wall-climbing cleaning robot cleans thoroughly. Compared to other methods, PCI considers amount and area occupation of different classes of dust. The dust data set is collected to train the designed model, and the model size is reduced to 14 % of the original model, and the FPS is 7.313 higher than the original model. Especially when compared with the state-of-the-art lightweight methods, our model has smaller model size and higher recognition speed. Experimental results have shown that our dust detection and cleanliness assessment method can be used on a wall-climbing cleaning robot to clean dust in time and thoroughly.

## 1. Introduction

In recent years, nuclear energy technology has been developing and the number of Nuclear Power Plants (NPP) has increased. However, the construction period of NPP is up to 5–6 years [1], and thick layer of dust accumulates on reactor containment after each step of the construction, especially the civil construction and installation steps [2]. In addition, during the running of the NPP, the reactor containment will also be attached with some dust deposited in the natural environment. These dust will become radioactive dust during the running of the NPP if they are not cleaned in time and thoroughly [3]. Radioactive dust will increase the difficulty of nuclear radiation protection and the risk of irradiation, endangering staff health and the environment [4]. The reactor containment dust may contain scattered dust, sticky dust and piles of dust that can be cleaned with different degrees of difficulty. The traditional visual inspection requires a large number of workers to observe continuously for a long period of time at a high altitude, and in this physically demanding and attention-consuming situation, visual errors can easily occur, leading to incomplete cleaning. Because of the

\* Corresponding author.

E-mail address: [13544903106@163.com](mailto:13544903106@163.com) (J. Zhu).

<https://doi.org/10.1016/j.heliyon.2024.e24220>

Received 28 August 2023; Received in revised form 11 December 2023; Accepted 4 January 2024

Available online 9 January 2024

2405-8440/© 2024 The Authors. Published by Elsevier Ltd. This is an open access article under the CC BY-NC-ND license (<http://creativecommons.org/licenses/by-nc-nd/4.0/>).

shortcomings of manual cleaning, the wall-climbing cleaning robot was put into use in NPP. However, early wall-climbing cleaning robots only route planning, do not distinguish between cleaning targets and cleanliness levels, resulting in blind cleaning, need for manual assistance, and low cleaning efficiency. Therefore, we would like to propose an algorithm that guides a wall-climbing cleaning robot to clean thoroughly and timely. This helps to prevent radioactive dust from being generated and reduces the need for dangerous high-altitude work by cleaning staff [5].

Traditional machine learning has been well studied in recognizing scattered dust [6–10], but it is mentioned in Ref. [11] that most of the machine learning methods deal with data in shallow structure. These structural models have only one or two layers of nonlinear feature transformation at most, while deep learning has more layers. So, when it comes to distinguishing differences in subcategories, deep learning is more accurate. In Ref. [12], researchers experimentally compared several traditional machine learning and deep learning models on different plant spots, and the experimental results showed that deep learning is more accurate and real-time than traditional machine learning. Combined with the above studies, we choose the deep learning method more appropriate when there are multiple types of morphological dust. In Ref. [13], the results of Faster Region-Convolutional Neural Network (Faster RCNN), You Only Look Once (YOLO) and Single Shot MultiBox Detector (SSD) were compared for recognizing images of fugitive dust, and YOLOv3 gave the best results. In Ref. [14], YOLOv5 was utilized to identify sand peaks and valleys to improve the efficiency of sand level positioning. In Ref. [15], state-of-the-art deep convolutional neural networks for image-based plant disease classification are fine-tuned and evaluated; Deep learning architectures are empirically compared. Experimental results show that the architecture performs well, but further research is needed to improve the computation time. The superiority of deep learning target detection algorithms can be seen from the above research, but as the algorithms continue to improve, the model complexity is also increased, and some algorithms only have theoretical effects and can not be practical application on mobile devices. Therefore, we need to make lightweight improvements of the selected algorithm.

The lightweight research of the detection model can effectively apply the theoretical algorithms to mobile devices in industrial life and improve the efficiency of mobile devices. In Ref. [16], ResNeXt model was parameterized as the backbone of the YOLOv5 model to improve the accuracy and speed of the YOLOv5 recognition fog installed in the vehicle; In Ref. [17], MobileNetV2 network architecture is used as a backbone for YOLOv3, and the improved model recognized tomato gray leaf spot disease with a 4-fold increase in speed; An improved garbage classification model based on ShuffleNetV2 is proposed in Ref. [18], which can be deployed on Raspberry Pi 4B to achieve fast detection of garbage classification. Knowledge distillation is used in Ref. [19] to help improve the adaptability of lightweight models with limited resources, while maintaining high-level representation capabilities.

The cleanliness evaluation criteria on the reactor containment are still mainly observed by human eyes, and there are no quantitative cleanliness evaluation criteria. The cleaning of sediment piles and sticky materials in road scenes is similar to the situation of dust spot and dust pile; therefore, we have investigated some road cleanliness assessment methods. Cleanliness Index (CI) is defined by the Spanish Federation of Municipalities and Provinces [20]. The assessment method considers factors such as the amount of garbage, the difficulty of removing garbage, climate and pavement conditions. After evaluation in real city streets and comparison with the population satisfaction method, positive results were obtained. The CI method only considers the amount and categories of garbage, not delicately consider the area ratio of the garbage. This method is not applicable to large areas of gravel on the roadway. To address this problem [21], proposed a cleanliness index based on semantic segmentation (CISS). CISS uses the area occupied by different categories of garbage to replace the amount of garbage in the CI method, and the area ratio of garbage in the image that can be easily obtained from the image segmentation result. Aiming at the advantages and disadvantages of these two methods, we combine the algorithm characteristics and propose a cleanliness assessment index named PCI that considers both the amount of targets and the area ratio of targets.

Summarizing the strengths and weaknesses of the above studies, the main contributions of our study can be summarized as follows.

- 1) A lightweight improved model based on YOLOv5s is proposed for mounting on a wall-climbing cleaning robot to recognize different categories of dust. Improvements are made by introducing shuffleNetV2 in the backbone part of YOLOv5s to reduce the model complexity, and adjusting the Loss function to improve to accuracy.
- 2) A cleanliness assessment method based on target detection is proposed. The method considers both target amount and area occupation, which can be used to judge the cleaning effectiveness of wall-climbing cleaning robots.

## 2. Reactor containment dust detection and cleaning system

The reactor containment dust detection and cleaning system in this paper mainly consists of camera, NVIDIA Jetson Xavier, water cannon, scraper and dust catcher. The dust detection and cleaning system works in the following steps.

- 1) The image of the current area is captured for the camera.
- 2) Jetson Xavier receives the image information and calls the S-YOLOv5 algorithmic model to detect whether the returned image contains targets to be cleaned.
- 3) if the current area contains 0 clean target, call the continue command; if the dust spot is detected, Jetson Xavier sends a signal to call the water cannon and scraper; if the dust pile is detected, Jetson Xavier sends a signal to call the dust catcher.
- 4) when the second case of the third step occurs, S-YOLOv5s will output the cleanliness evaluation parameter when it receives the cleaning completion signal. If the cleanliness level does not reach "high", repeat steps 1, 2, and 3 until the cleanliness is "High" and then move on to the next area.

The dust detection and cleaning system structural framework is shown in Fig. 1.

### 3. S-YOLOv5s dust detection algorithm

The detection speed of YOLOv5s is greatly improved compared to the two-stage detection network Faster-RCNN [22], and compared to the SSD algorithm [23], which is also a single-stage target detection, the size of the YOLOv5s model is less than one-tenth of the size of the SSD model, which requires low hardware capability, and is more suitable for deploying to mobile devices. Despite the small size of the YOLOv5s model, it suffers from lag when deployed on the wall-climbing robot. In order to solve this problem, this paper proposes to lightweight the model.

ShuffleNetV2 is a lightweight network architecture. In the ShuffleNetV2 paper [24], four criteria for lightweight are proposed.

- 1) Equal channel width minimizes memory access cost (MAC).
- 2) Excessive group convolution increases MAC.
- 3) Network fragmentation reduces degree of parallelism.
- 4) Element-wise operations are non-negligible.

In order to fulfill these four criteria, ShuffleNetV2 introduce a simple operator called channel split. It is illustrated in Fig. 2 (a). At the beginning of each unit, the input of feature channels are split into two branches with two channels, respectively. Following criteria 3, one branch remains as identity. The other branch consists of three convolutions with the same input and output channels to satisfy criteria 1. The two  $1 \times 1$  convolutions are no longer group-wise. This is partially to follow criteria 2, an partially because the split operation already produces two groups.

After convolution, the two branches are concatenated. So, the number of channels keeps the same. The same “channel shuffle” operation then used to enable information communication between the two branches.

After the shuffling, the next unit begins. Note that the “Add” operation no longer exists. Element-wise operations like ReLU and depth-wise convolutions exist only in one branch. Also, the three successive element-wise operations, “Concat”, “Channel Shuffle” and “Channel Split”, are merged into a single element-wise operation. These changes are beneficial according to criteria 4.

For spatial down sampling, the unit is slightly modified and illustrated in Fig. 2 (b). The channel split operator is removed. Thus, the number of output channels is doubled.

The ShuffleNetV2 structure is as follows.

Because of all the above advantages, we introduce ShuffleNetV2 as the backbone of the S-YOLOv5s model. ShufflenetV2 controls equal channel widths and reduces group convolution and fragmentation compared to CSPDarknet, resulting in a reduction of the model size and memory access cost, an increase in the degree of network parallelism, and an increase in the speed of detection when deployed on mobile devices.

After lightweight, the accuracy of the algorithm decreases, in order to balance the speed and accuracy, this paper replaces the loss function of the prediction part of YOLOv5s from CIoU [25] to Siou [26].

The CIoU used by YOLOv5s is defined as Equations (1)–(4):

$$R_{CIoU} = IoU - \frac{\gamma^2(b, b^{gt})}{c^2} + \alpha v \quad (1)$$

$$L_{CIoU} = 1 - IoU + R_{CIoU} \quad (2)$$

$$\alpha = \frac{v}{(1 - IoU) + v} \quad (3)$$

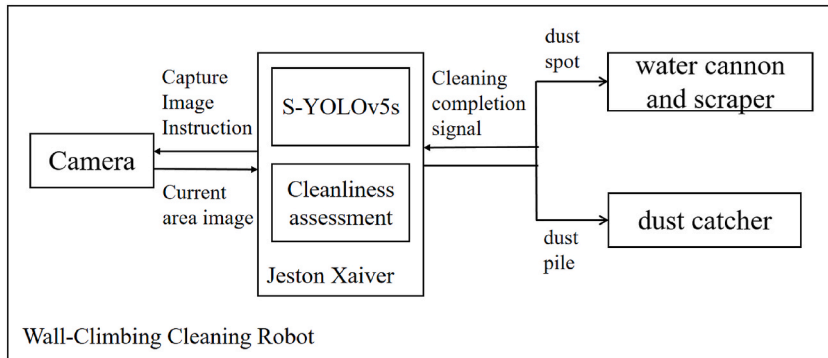


Fig. 1. Dust detection and cleaning system.

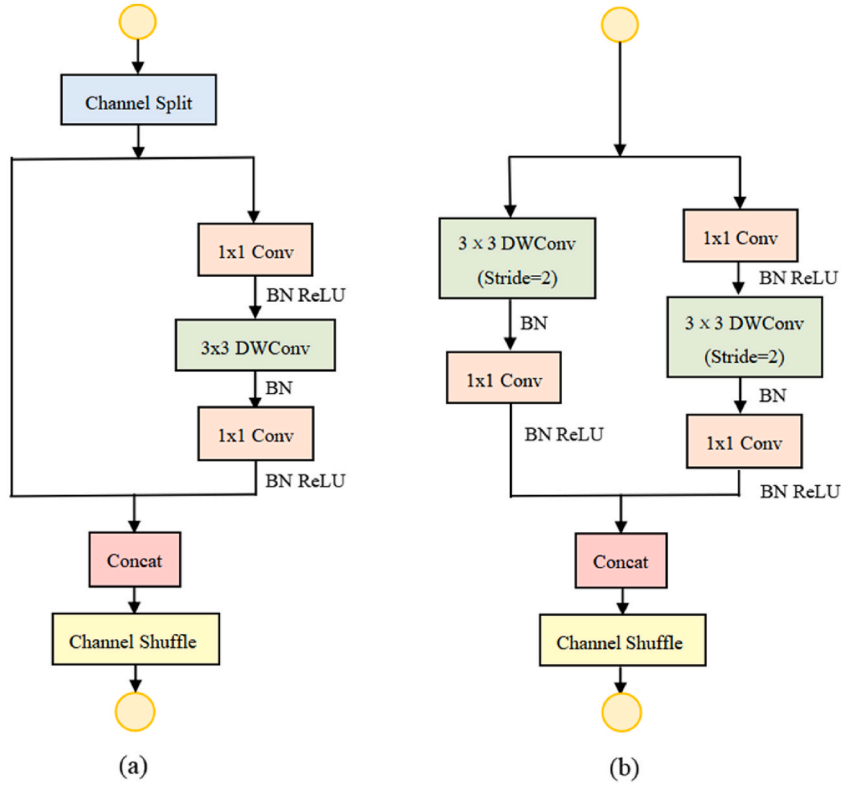


Fig. 2. ShuffleNetV2 structure. (a) is the basic unit of ShuffleNetV2; (b) is the spatial down sampling unit of ShuffleNetV2.

$$v = \frac{4}{\pi^2} \left( \arctan \frac{w^{gt}}{h^{gt}} - \arctan \frac{w}{h} \right)^2 \quad (4)$$

$\gamma^2(b, b^{gt})$  denotes the Euclidean distance between the centroid of the prediction box and the centroid of the actual box,  $\alpha$  denotes the shortest diagonal length of the minimum enclosing box of the prediction box and the ground truth box,  $v$  is a positive balance parameter indicating the consistency of the prediction box with the aspect ratio of the ground truth box.

Among them, IoU [27] is defined as Equation (5):

$$IoU(B, B^{gt}) = \frac{|B \cap B^{gt}|}{|B \cup B^{gt}|} \quad (5)$$

It can be seen that CIoU, although highly focused on bounding box shapes does not take into account the matching of directions between the prediction box and the target box, and is computationally complex. SIoU considers the angle cost thus addressing the slower convergence due to the above shortcomings.

Distance cost and shape cost after considering angle cost in SIoU are defined as Equations (6) and (7):

$$\Omega = \sum_{t=w,h} (1 - e^{-wt})^\theta \quad (6)$$

$$\Delta = \sum_{t=x,y} (1 - e^{-\gamma \rho t}) \quad (7)$$

In (6),  $\omega_w = \frac{|w-w^{gt}|}{\max(w,w^{gt})}$ ,  $\omega_h = \frac{|h-h^{gt}|}{\max(h,h^{gt})}$ ,  $\theta$  control shape cost  $\Omega$  importance.

In (7),  $\rho_x = \left( \frac{b_{cx}^{gt} - b_{cx}}{c_w} \right)$ ,  $\rho_y = \left( \frac{b_{cy}^{gt} - b_{cy}}{c_w} \right)$ ,  $\gamma = 1 + 2 \sin^2 \left( \sin^{-1} \frac{|b_{cy}^{gt} - b_{cy}|}{\sqrt{(|b_{cx}^{gt} - b_{cx}|)^2 + (|b_{cy}^{gt} - b_{cy}|)^2}} - \frac{\pi}{4} \right)$ .

Final SIoU is defined as Equation (8):

$$L_{Siou} = 1 - IoU + \frac{\Delta + \Omega}{2} \quad (8)$$

Angular penalty cost effectively reduces total number of degrees of freedom. The prediction box is directly close to the X-axis or Y-axis of the real box, and then continues to be close to it along the correlation axis, which speeds up the convergence of the network, and

further improves the regression accuracy.

After completing the above improvements, the S-YOLOv5s dust detection algorithm model with balanced accuracy and speed is obtained. The structure of the S-YOLOv5s model is shown in Fig. 3.

#### 4. PCI cleanliness assessment method

The cleanliness of the reactor containment is still judged by human eyes to determine whether it has reached a clean level, and there is no research in the evaluation method applicable to wall-climbing cleaning robots. On road scenarios similar to the setting of this paper, CI is defined by the Spanish Federation of Municipalities and Provinces in its Guía Técnica para la Gestión de Residuos Municipales y Limpieza Viaria (Technical Guide for Municipal Waste Management and Street Cleaning) and we use it as a reference. CI is a cleanliness assessment method that uses the amount and type of road garbage as the main criterion, The CI is defined as Equation (9) :

$$CI = \frac{\gamma}{n} \sum_{i=0}^K \frac{W_i}{S} \times 100 \tag{9}$$

$\gamma$  and  $n$  are correction coefficients.  $\gamma$  takes into account the damage of the ground,  $n$  is the sudden change of the number of garbage in special cases,  $K$  denotes the total number of garbage categories,  $i$  is the category number of garbage,  $W_i$  is the weighted amount of garbage of category  $i$ , and  $S$  is the observation area.

And the categories and weights related to dust in the CI method are shown in the following Table 1.

Table 1 show that CI only roughly divides the area occupation of inorganic waste into three levels of small, medium and large, and Sticky residues have only one weight value regardless of size. CI will show the same cleanliness level when evaluating the same amount and the same category of targets with different area occupation. It is clear that CI is not suitable for assessing targets that require careful differentiation of area occupation, such as dust and sand.

When defining the weight values of the targets, we no longer distinguish between small, medium and large, but only between dust categories. Then, the area ratio is further subdivided. PCI corresponding weights for each category are shown in Table 2 below.

Since the reactor containment surface is generally smooth and the dust does not change suddenly, we do not consider  $\gamma$  and  $n$ . Further, we use the percentage of target box area output from the S-YOLOv5s algorithm as one of the cleanliness assessment factor, and add  $n$  to indicate the number of targets of each category in the current area. Finally we obtain the PCI assessment criteria as shown in Equation (10):

$$PCI = \sum_{i=0}^K P_i B_i \times 100 + n_i \tag{10}$$

$K$  denotes the total number of target categories,  $P_i$  is the percentage of target box area in category  $i$ , it replaces  $\frac{1}{3}$  in CI,  $B_i$  is the weight of targets in category  $i$ , it replaces  $W_i$  in CI,  $n_i$  is the number of targets in category  $i$ .

The inclusion of the target frame area share adjusted the cleanliness index classification levels accordingly, as shown in Table 3.

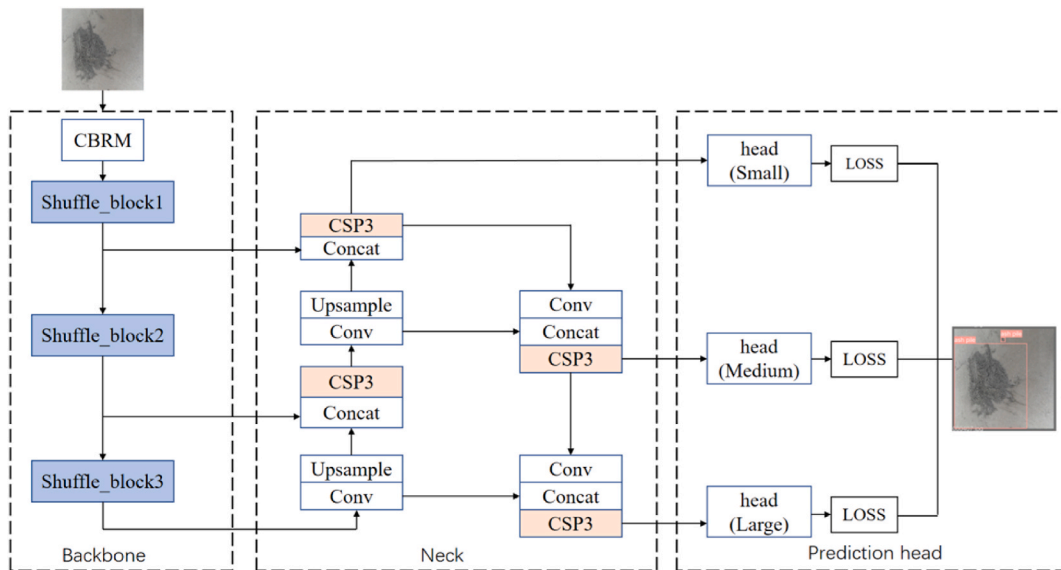


Fig. 3. S-YOLOv5s structure.

**Table 1**  
Table of weights for CI categories.

Category name		weight value
Inorganic rubbish	Small	1
	Medium	2
	Large	4
Sticky residue		2

**Table 2**  
Table of weights for PCI categories.

Category name	weight value
Reflection	0
Dust pile	1
Dust spot	2

## 5. Experiments and analyses

### 5.1. Experimental setup and data set

#### 5.1.1. Experimental setup and evaluation metrics for the model

We train the dust recognition model in Centos7 based on Python code and Pytorch [28] framework. The hardware configuration is as follows: two NVIDIA's A100 graphics cards, Intel(R) Xeon(R) Gold 6226R CPU @ 2.90 GHz processor. The proposed method is trained for 300 cycles at an initial learning rate of 0.01 with a training momentum of 0.937, a weight decay parameter of 0.0005, and a training batch of four. The validation phase deploys the model on a Jeston Xavier wall-climbing cleaning robot and records the real-time detection effect and detection speed.

The evaluation metrics of the model include **mAP@0.5**, Model Size(MB),FPS and GFLOPS.

**mAP@0.5**: average accuracy for all categories with IoU threshold set to 0.5.

**Model Size**: The size of the memory occupied by the model in the device.

**FPS**: Frames per second transmitted.

**GFLOPS**: Number of floating point operations per second in billions.

#### 5.1.2. Collection of data set

The data set portion is primarily indoor and outdoor dusty wall surfaces.

Due to the vacancy of dust images on the reactor containment wall after the construction was completed. We collected indoor and outdoor dust spots and dust piles from the post-construction site for different lighting images. During the data collection process, it was found that smooth surfaces such as metal surfaces would have light reflections in the lighting environment, which would cause some interference with other category identification, so the reflection were also divided into a separate category.

The total number of images in the data set and the number of labels per category are shown in Table 4.

### 5.2. Validation of the S-YOLOv5s model

#### 5.2.1. Ablation experiment

In order to verify the effectiveness of our two-part improvement of YOLOv5s, we did 3 sets of comparison experiments. The added modules are represented by " $\sqrt$ ".

- ① Comparison of each evaluation parameter before and after backbone replacement.
- ② Comparison of each evaluation parameter before and after loss function replacement only.
- ③ Comparison of each evaluation parameter between original YOLOv5s and S-YOLOv5s.

The experimental results are shown in Table 5, and the added modules are represented by " $\sqrt$ ".

**Table 3**  
Table of cleanliness index levels.

Cleanliness index	Cleanliness level	Numerical level
$PCI < 8$	high	1
$8 \leq PCI < 19$	medium	2
$19 \leq PCI < 30$	low	3
$PCI \geq 30$	Very low	4

**Table 4**  
Dataset image volume and number of tags per category.

	dust spot	dust pile	reflection
Amount of labels	553	286	158
Total amount of pictures	506		

The accuracy ( $mAP@0.5$ ), model size, operational operands required by the model (GFLOPS) and recognition speed (FPS) were compared before and after each improvement. As can be seen from the results in Table 5, replacing the loss function CIoU of the original network with SIoU, the  $mAP@0.5$  and the FPS are improved by 2.3 % and 3.405, respectively. This can indicate that the SIoU plays a role in improving the accuracy and increasing the speed of detection. After replacing the backbone with ShuffleNetV2, the FPS are improved by 5.44, the  $mAP@0.5$ , size and operational operands of the model were reduced by 17.3 %, 11.78 MB, and 14, respectively. It can be seen that ShuffleNetV2 makes the model accuracy decrease, but speeds up the model detection and reduces the model size and complexity. Adding SIoU on top of the ShuffleNetV2 improvement, the  $mAP@0.5$  and the FPS increased by 5.4 % and 1.873, respectively, while maintaining the same model size and operational operands. This shows that SIoU is better at improving accuracy when the backbone is ShuffleNetV2.

### 5.2.2. Comparative experiments with other models

We compare the accuracy and recognition speed of the S-YOLOv5s algorithm with the original algorithm, SSD, Faster-RCNN, and other YOLO models of similar size. The results are shown in Table 6.

Before improvement, the model size of YOLOv5s is 13.7 MB, which is smaller than other models except YOLOv6n, YOLOv7-tiny, and YOLOv8n; The FPS is higher than all models except SSD; And, the  $mAP@0.5$  is 92 %, which is the highest among all models. In summary, YOLOv5s is the model that best balances accuracy and detection speed. After lightweight improvements to the YOLOv5s, S-YOLOv5s model has the smallest size, with a Model Size of 1.92 MB, and the fastest detection speed, with an FPS of 56.818. Compared with YOLOv4-tiny, YOLOv6n, YOLOv7-tiny, SSD and Faster-RCNN models,  $mAP@0.5$  increases by 15.7 %, 29.8 %, 28.3 %, 12.3 %, 49.5 % respectively. Although  $mAP@0.5$  is 8.2 %, 11.9 %, and 0.5 % lower than YOLOv3-Tiny, YOLOv5s and YOLOv8n, respectively, S-YOLOv5s consumes less device memory, which is friendly to some mobile devices with only 8-16G RAM.

ShuffleNetV2 has a large number of equal-width channels, a small number of convolutional groupings, a "Channel Shuffle" branching communication method, and an efficient element algorithm, which serves to improve the speed of model detection and reduce the model size and model complexity. And the angle penalty mechanism of SIoU improves the accuracy of model detection. This is why the S-YOLOv5s is able to recognize dust faster.

### 5.3. Test set testing and real-time inspection

Some of the detection results of the S-YOLOv5 model for the test set are shown in Fig. 4.

It can be seen that the model is generally better for category detection, the target box is accurate. The hindrance of reflections to dust recognition is reduced by giving reflections a separate classification. Accuracy for each category on the test set was 81.8 % for dust spot, 82.1 % for dust piles, and 76.5 % for reflections. Because the number of reflection samples is relatively small, the accuracy of reflections is slightly lower.

Deploying the S-YOLOv5s model to the Jeston Xavier wall-climbing cleaning robot, the real-time detection speed on the lab wall can reach up to 27 frames/s, and some of the real-time detection results are shown in Fig. 5.

### 5.4. Cleanliness assessment model validation

When calculating CI based on the original image, the objects in our image generally do not have a sudden change in number and the plane is smooth, so set  $\lambda = 1$ ,  $n = 1$ , the detection range is 1 square meter, set  $S = 1$ , and in accordance with the weight values in Table 1, the dust spot calculates the weights according to the viscous residue, and the dust pile calculates the weights according to the inorganic garbage. When calculating the PCI, according to the weight values Table 2, weight value of dust spot is 2, weight value of dust pile is 1, and weight value of reflective is 0. Other parameters are output according to the target detection algorithm.

We selected different experimental samples as examples for evaluation. These samples were evaluated by the CI and PCI methods. It can be seen that the two methods have different cleanliness level evaluation results on several samples, as shown in the following Fig. 6.

**Table 5**  
Table of comparison of results of ablation experiments.

Experiment number	CSPDarknet53	ShuffleNet V2	CIoU	SIoU	$mAP@0.5$	Model Size(MB)	GFLOPS	FPS
1	✓		✓		0.920	13.7	15.8	49.505
2	✓			✓	0.943	13.7	15.8	52.910
3		✓	✓		0.747	1.92	1.8	54.945
ours		✓		✓	0.801	1.92	1.8	56.818

**Table 6**

Table of results comparing YOLOv5s model with other models.

Model	Backbone	Model Size(MB)	Map@0.5	FPS
YOLOv3-tiny	Darknet53	16.6	0.883	21.645
YOLOv4-tiny	CSPDarknet53	22.4	0.644	42.751
YOLOv5s	CSPDarknet53	13.7	0.920	49.505
YOLOv6n	EfficientRap	9.94	0.503	19.56
YOLOv7-tiny	Darknet53	12.3	0.518	9.98
YOLOv8n	Darknet53	5.95	0.806	31.150
SSD	MobileNetV2	15.3	0.678	54.487
Faster-RCNN	ResNet50	108	0.306	35.873
ours	ShuffleNetV2	1.92	0.801	56.818

**Fig. 4.** Some test results of the test set images.

We refine the consideration of dust area occupancy by using target box area ratio and add a target amount factor, which results in a more accurate assessment of the cleanliness rating of dusty surfaces. The cleanliness of reactor containment in NPP is still based on the subjective judgment of cleaning staff. The cleaners use the size, amount and adhesion of dust to determine whether the current area is clean or not. So, we gave the cleaner before and after pictures to judge the cleanliness level, and the standard we got was basically the same as the evaluation result from our assessment method. In particular, the cleaners gave the same conclusions for the pictures with high and very low cleanliness levels, but the conclusions between medium and high levels were partially inconsistent.

## 6. Conclusion and future work

Because of the hardware resource limitations of the wall-climbing cleaning robot, models with high complexity are limited in detection speed or even unable to run on the wall-climbing robot. To solve this problem, ShuffleNetV2 is introduced in YOLO v5s as a backbone to reduce the model complexity. As many feature layers are cut, the accuracy is reduced. In order not to deepen the network and maintain the detection accuracy above 80 %, we adjust the loss function to improve the accuracy. Compared to the original YOLOv5s, the model size of S-YOLOv5s is reduced to 14 % of the original model, the accuracy is maintained at 80.1 %, and the detection frame rate is faster by 7.313 frames/s, which enables real-time detection on wall-climbing robots as well. Compared with other methods, S-YOLOv5s has smaller model size and detection speed. In addition, the factors that the human eyes use to judge cleanliness levels (area and amount of dust) are quantified. In this way, PCI can be used in conjunction with the recognition algorithm to ensure that the wall-climbing robot thoroughly clean. Experiments show that dusty spots can be confused with other spots of similar color. We presume that S-YOLOv5s recognition dust spots mostly relies on color features. How to improve the multi-feature convergence ability of the algorithm while keeping the model lightweight is what we need to continue to research and explore.





## Funding information

Science and Technology Major Project of Fujian Province (No.2021R106006, No.JAT200345); Inner Mongolia Autonomous Region Science and Technology Project (No.2023YFSW0020).





Fig. 5. Real-time detection of effects.

Different test samples				
CI	300	600	1000	400
cleanliness level	Very low	Very low	Very low	Very low
PCI	41.99	13.60	24.89	12.48
cleanliness level	Very low	Medium	Low	Medium




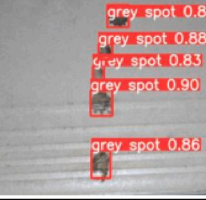
不同检测样本				
CI	600	600	300	1000
cleanliness level	Very low	Very low	Very low	Very low
PCI	6.11	7.96	46.04	14.15
cleanliness level	High	High	Very low	Medium

Fig. 6. Results of CI and PCI assessment of different experimental samples.

## Data availability

The data that support the findings of this study are available in dust-data-set-and-S-YOLOv5s at: <https://github.com/Applee12304/dust-data-set-and-S-YOLOv5s/tree/master>.

## CRediT authorship contribution statement

**Li-Wen Chen:** Writing – review & editing, Supervision, Investigation, Funding acquisition, Conceptualization. **Jing Zhu:** Writing – original draft, Visualization, Validation, Software, Methodology, Investigation, Data curation. **Huanghui Zhang:** Supervision, Resources, Formal analysis, Data curation. **Yang Liu:** Supervision, Investigation, Formal analysis, Conceptualization. **Chun-yu Liu:** Writing – review & editing, Supervision, Resources, Investigation, Data curation.

## Declaration of competing interest

The authors declare the following financial interests/personal relationships which may be considered as potential competing interests: The authors declare the following financial interests/personal relationships which may be considered as potential competing interests: Li-Wen Chen reports financial support was provided by Science and Technology Major Project of Fujian Province (No.2021R106006, No.JAT200345); Inner Mongolia Autonomous Region Science and Technology Project (No.2023YFSW0020).

## References

- [1] Sui Yang, Rui Ding, Hanqing Wang, A novel approach for occupational health and safety and environment risk assessment for nuclear power plant construction project, *J. Clean. Prod.* 258 (2020) 120945, <https://doi.org/10.1016/j.jclepro.2020.120945>.
- [2] Mingpu Wang, Gang Yao, Yujia Sun, Yang Yang, Rui Deng, Exposure to construction dust and health impacts-A review, *Chemosphere* 311 (2023) 136990, <https://doi.org/10.1016/j.chemosphere.2022.136990>.
- [3] Gyoung G. Jang, Alexander I. Wiechert, Yong-Ha Kim, Austin P. Ladshaw, Spano Tyler, Joanna McFarlane, Kristian Myhre, Joon Jin Song, Sotira Yiacoymi, Costas Tsouris, Charging of radioactive and environmental airborne particles, *J. Environ. Radioact.* 248 (2022) 106887, <https://doi.org/10.1016/j.jenvrad.2022.106887>.
- [4] J. P. Sharpe, D.A. Petti, H.-W. Bartels, A review of dust in fusion devices: implications for safety and operational performance, *Fusion Eng. Des.* 63–64 (2002) 153–163, [https://doi.org/10.1016/S0920-3796\(02\)00191-6](https://doi.org/10.1016/S0920-3796(02)00191-6).
- [5] Mohammad Z. Shanti, Chung-Suk Cho, Borja Garcia de Soto, Young-Ji Byon, Chan Yeob Yeun, Tae Yeon Kim, Real-time monitoring of work-at-height safety hazards in construction sites using drones and deep learning, *J. Saf. Res.* 83 (2022) 364–370, <https://doi.org/10.1016/j.jsr.2022.09.011>.
- [6] Z. Yubo, Z. Yadong, Z. Bin, Desktop dust detection algorithm based on gray gradient co-occurrence matrix, *J. Comput. Appl.* 39 (8) (2019) 2414, <https://doi.org/10.11772/j.issn.1001-9081.2019010081>.
- [7] O.A. Arqub, Z. Abo-Hammour, Numerical solution of systems of second-order boundary value problems using continuous genetic algorithm, *Inf. Sci.* 279 (2014) 396–415, <https://doi.org/10.1016/j.ins.2014.03.128>.
- [8] A. Proietti, M. Panella, F. Lecce, E. Svezia, Dust detection and analysis in museum environment based on pattern recognition, *Measurement* 66 (2015) 62–72, <https://doi.org/10.1016/j.measurement.2015.01.019>.
- [9] Z. Abo-Hammour, O.A. Arqub, S. Momani, N. Shawagfeh, A. Tersian, Stepan, Optimization solution of troesch's and bratu's problems of ordinary type using novel continuous genetic algorithm, *Discrete Dynam Nat. Soc.* 2–9 (2014) 401696, <https://doi.org/10.1155/2014/401696>.
- [10] O.A. Arqub, Z. Abo-Hammour, M. Shaher, N. Shawagfeh, Solving singular two-point boundary value problems using continuous genetic algorithm, *Abstr. Appl. Anal.* 5 (2012) 205391, <https://doi.org/10.1155/2012/205391>.
- [11] P. Wang, F. En, W. Peng, Comparative analysis of image classification algorithms based on traditional machine learning and deep learning, *Pattern Recogn. Lett.* 141 (2021) 61–67, <https://doi.org/10.1016/j.patrec.2020.07.042>.
- [12] J.A. Wani, S. Sharma, M. Muzamil, et al., Machine learning and deep learning based computational techniques in automatic agricultural diseases detection: methodologies, applications, and challenges, *Arch. Comput. Methods Eng.* 29 (1) (2022) 641–677, <https://doi.org/10.1007/s11831-021-09588-5>.
- [13] R. Xiong, P. Tang, Machine learning using synthetic images for detecting dust emissions on construction sites, *Smart and Sustainable Built Environment* 10 (3) (2021) 487–503, <https://doi.org/10.1108/SASBE-04-2021-0066>.
- [14] M. Liu, S. Yue, S. Li, Y. Du, B. Li, Research on intelligent detection of concrete aggregate level based on monocular imaging, *Measurement* 194 (2022) 111036, <https://doi.org/10.1016/j.measurement.2022.111036>.
- [15] E.C. Too, L. Yujian, S. Njuki, L. Yingchun, A comparative study of fine-tuning deep learning models for plant disease identification, *Comput. Electron. Agric.* 161 (2019) 272–279, <https://doi.org/10.1016/j.compag.2018.03.032.J>.
- [16] H. Wang, Y. Xu, Y. He, Y. Cai, L. Chen, Y. Li, M.A. Sotelo, Z. Li, YOLOv5-Fog: a multiobjective visual detection algorithm for fog driving scenes based on improved YOLOv5, *IEEE Trans. Instrum. Meas.* 71 (2022) 1–12, <https://doi.org/10.1109/TIM.2022.3196954>.
- [17] Liu, X. Wang, Early recognition of tomato gray leaf spot disease based on MobileNetV2-YOLOv3 model, *Plant Methods* 16 (2020) 1–16, <https://doi.org/10.1186/s13007-020-00624-2>.
- [18] Z. Chen, J. Yang, L. Chen, H. Jiao, Garbage classification system based on improved ShuffleNet v2, *Resour. Conserv. Recycl.* 178 (2022) 106090, <https://doi.org/10.1016/j.resconrec.2021.106090>.
- [19] Y. Wang, Y. Wang, J. Cai, et al., Ssd-kd: a self-supervised diverse knowledge distillation method for lightweight skin lesion classification using dermoscopic images, *Med. Image Anal.* 84 (2023) 102693, <https://doi.org/10.1016/j.media.2022.102693>.
- [20] Sevilla, M.L. Rodríguez, Á. García-Maraver, M. Zamorano, An index to quantify street cleanliness: the case of Granada (Spain), *Waste Manag.* 33 (5) (2013) 1037–1046, <https://doi.org/10.1016/j.wasman.2013.01.012>.
- [21] Liao, X. Luo, L. Cao, W. Li, X. Feng, J. Li, F. Yuan, Road garbage segmentation and cleanliness assessment based on semantic segmentation network for cleaning vehicles, *IEEE Trans. Veh. Technol.* 70 (9) (2021) 8578–8589, <https://doi.org/10.1109/TVT.2021.3100264>.
- [22] S. Ren, K. He, R. Girshick, J. Sun, Faster R-CNN: towards real-time object detection with region proposal Networks, in: *IEEE Trans. Pattern Anal. Mach. Intell.* 39 (6) (2017) 1137–1149.
- [23] W. Liu, D. Anguelov, D. Erhan, C. Szegedy, S. Reed, C.Y. Fu, A.C. Berg Ssd, Single shot multibox detector, in: *Computer Vision—ECCV 2016: 14th European Conference vol. 14*, Springer International Publishing, Amsterdam, The Netherlands, 2016, pp. 21–37. October 11–14, 2016, Proceedings, Part I.
- [24] N. Ma, X. Zhang, H.T. Zheng, J. Sun, Shufflenet v2: practical guidelines for efficient cnn architecture design, in: *Proceedings of the European Conference on Computer Vision, ECCV*, 2018, pp. 116–131.
- [25] Z. Zheng, P. Wang, W. Liu, J. Li, R. Ye, D. Ren, Distance-IoU loss: faster and better learning for bounding box regression, in: *Proceedings of the AAAI Conference on Artificial Intelligence vol. 34*, 2020, pp. 12993–13000. No. 07.

- [26] Z. Gevorgyan, SloU Loss: More Powerful Learning for Bounding Box Regression, 2022, <https://doi.org/10.48550/arXiv.2205.12740> arXiv preprint arXiv: 2205.12740.
- [27] J. Yu, Y. Jiang, Z. Wang, Z. Cao, T. Huang Unitbox, An advanced object detection network, in: *Proceedings of the 24th ACM International Conference on Multimedia*, 2016, pp. 516–520.
- [28] A. Paszke, S. Gross, F. Massa, A. Lerer, J. Bradbury, G. Chanan, S. Chintala, PyTorch: an Imperative Style, High-Performance Deep Learning Library, 2019, <https://doi.org/10.48550/arXiv.1912.01703> arXiv e-prints, arXiv-1912.